

# Morphological, Chemical, and Mechanical Characterization of Untreated and Mercerized Lignocellulosic Fibers

David Uriel Jayson B. Bas<sup>1\*</sup>, Vera Karla S. Caingles<sup>1</sup>

Dave Joseph E. Estrada<sup>1</sup>, and Cheryl F. Daleon<sup>2</sup>

<sup>1</sup>Civil Engineering Department

University of Science and Technology of Southern Philippines

Alubijid, Misamis Oriental, 9018 Philippines

\*[davidurieljayson.bas@ustp.edu.ph](mailto:davidurieljayson.bas@ustp.edu.ph)

<sup>2</sup>Civil Engineering Department

Central Mindanao University

Maramag, Bukidnon, 8714 Philippines

Date received: August 29, 2025

Revision accepted: December 12, 2025

---

## Abstract

*The exponential increase in carbon emissions has prompted a deviation from natural fibers as an alternative to synthetic materials. Bamboo culms, pineapple leaves, and coconut husks contain lignocellulosic fibers that can be used in biocomposite and geotextile applications. Hence, this study aimed to determine the surface morphology, mean diameter, porosity, chemical composition, and tensile strength of untreated and alkali-treated fibers, with 6% sodium hydroxide used for treatment. Results revealed that mercerization enhanced the fibers' adhesion and restructured the fractured fragments of the fibers' microstructure. Moreover, the FTIR results showed an improved cellulose content in the treated lignocellulosic fibers. Mercerized bamboo fibers contain the highest cellulose content at a critical peak of 3389  $\text{cm}^{-1}$ , while treated coconut fibers yield the lowest cellulose content at an absorption peak of 3339  $\text{cm}^{-1}$ . Conversely, treated bamboo fibers yield the highest tensile strength of 23.6897 MPa (a 90.43% increase), while treated coconut fibers yield the lowest tensile strength of 2.0389 MPa (a 10.87% increase). In conclusion, the mercerization of fibers improves surface morphology, cellular composition, and mechanical strength.*

**Keywords:** lignocellulosic fibers, mercerization, morphology, sodium hydroxide, tensile strength

---

## 1. Introduction

In recent years, the growing emphasis on environmental sustainability has prompted a contemporary impetus towards natural fibers as an eco-friendly

alternative to synthetic counterparts (Hindi *et al.*, 2025). With the escalating concerns about the environmental impact of synthetic geotextiles, such as high carbon emissions and long-term soil and landfill pollution, the emergence of lignocellulosic fibers, such as bamboo, pineapple, and coconut, has been discerned as ideal geotextile alternatives for soil stabilization and erosion control (Kumar, 2023).

Bamboo is a renewable material that has enhanced mechanical properties due to its unidirectional fiber arrangement and cellulose composition (Hawanis *et al.*, 2024). Recent research revealed the utilization of bamboo fibers in the production of polymer matrix composites, wherein its tensile strength had a significant improvement of 66% (dos Santos *et al.*, 2024). Another study exhibited the effectiveness of bamboo geotextiles in improving the bearing capacity of dispersive soils, as the ultimate bearing capacity of soil in Kalangan Hamlet, Indonesia, had a 234.43% increase (Pinka *et al.*, 2021). Conversely, pineapple leaf fibers are composed of inherent rigidity and exceptional flexural and torsional properties due to the high crystallinity of their cellulosic microfibrils (Sebastian and Divya, 2024). A study conducted by Balbin *et al.* (2022) revealed that pineapple leaf fiber geotextile has enhanced mechanical properties compared to the commercially available coconut, as its tensile strength increased by 29.01%. Additionally, its water absorption rate has increased by 30.42%, making it effective in reducing subsequent slope failure and soil erosion. In the Philippines, a study conducted by Caingles and Lira (2025) revealed that pineapple-coconut net geotextile has increased the runoff and soil loss reduction effectiveness by 105%, making it effective in controlling soil loss. Moreover, coconut fibers have a high lignin content and are abrasion-resistant (Sebastian and Divya, 2024). A recent study revealed that coconut geotextiles have been used to enhance drainage for soil consolidation and prevent lateral deformation and collapse (Nguyen and Indraratna, 2023). Another study revealed that treated single-layer and double-layer coir geotextiles have increased the California bearing ratio of organic clayey soil by 5.94% and 10.31%, respectively, highlighting their effectiveness in the construction of durable pavements and embankments (Bawadi *et al.*, 2025).

Despite the promising results of these fibers, their sustainability has had drawbacks for long-term applications under extreme environmental conditions, including heatwaves and drought, as well as heavy rainfall and flooding (Tanasă *et al.*, 2022). Thus, the mercerization of fibers for surface modifications is performed to improve their mechanical interlocking with the

polymer matrix, thereby enhancing their tensile strength properties (Li *et al.*, 2025). Hence, this study employed a 6% NaOH solution, which is consistent with earlier literature that cites it as the optimal concentration. Holanda *et al.* (2024) elucidated that a 6% NaOH treatment is the optimal concentration to improve the tensile strength of *Typha domingensis* fibers against field degradation over a period exceeding 180 days. Another study showed that a 6% treated pineapple leaf fiber net displayed a higher tensile strength of 6.79 MPa than the commercially available coconet of 4.82 MPa (Balbin *et al.*, 2022). In consonance with the study of Jena *et al.* (2024), alkali-treated geotextiles achieved a 54.90% increase in mean tensile strength, thus improving mechanical properties. Moreover, Sachin Chakravarthy *et al.* (2021) revealed that alkali-activated binder-treated jute geotextiles showed a 120.18% increase in average tensile strength.

However, there remains insufficient quantitative discussion on how a standardized 6% NaOH concentration simultaneously influences the chemical composition, surface morphology, mean diameter, porosity, and tensile strength of different tropical fibers. The existing literature often lacks an integrated analysis combining FTIR, SEM, and physical property evaluations, which are essential to correlate chemical changes with morphological and mechanical improvements. Therefore, there is a research gap in establishing a comparative, systematic evaluation of the physicochemical responses of bamboo, coconut, and pineapple fibers to a moderate 6% NaOH treatment, which could serve as a standardized and sustainable pretreatment protocol for multi-fiber biocomposite applications. Furthermore, this study investigated the potential of lignocellulosic fibers in sustainable geotechnical applications. Specifically, this study aimed to: determine the surface morphology, mean diameter, and porosity of untreated and mercerized lignocellulosic fibers; determine the cellulosic composition of control and treated fibers; and determine the tensile strength of untreated and mercerized fibers.

## **2. Methodology**

### *2.1 Materials*

The pineapple leaves were collected from the Pineapple Plantation of Delmonte Pineapple Philippines Inc. in Impasug-ong, Bukidnon. These leaves are within 1.2–1.5 years, which is the harvest time for pineapple plants. Leaves

harvested from plants aged 12 to 18 months yield fibers with superior strength and pliability compared to those from younger or over-mature plants (Tulin and Bande, 2018). Meanwhile, the bamboo fibers were sourced and extracted from mature bamboo culms in Barangay Simbalan, Buenavista, Agusan del Norte, with an age of 2 to 3 years due to the presence of culm sheaths and nodal rings (Dessalegn *et al.*, 2022). According to the study of Singh *et al.* (2023), this is the ideal age for bamboo fiber extraction as its cell wall thickening is complete, resulting in an ideal amount of cellulose and amorphous lignin due to its higher respiration rate. Additionally, the coconut fibers made from coconut husk were procured at Malingao Community Service Multipurpose Cooperative (MCOCO) in Lanao del Norte. Furthermore, the sodium hydroxide (industrial grade) was procured in La Victoria, Cogon, Cagayan de Oro City.

## 2.2 Mercerization of Fibers

This research has incorporated the study of Balbin *et al.* (2022) and Holanda *et al.* (2024), wherein a 6% NaOH solution was used for the treatment of specimens. On 5 liters of distilled water with 300g of NaOH, the lignocellulosic fibers were soaked for 24 hours. Hence, the molarity is a 1.5 M NaOH solution. Thereafter, the fibers were washed thoroughly with water to neutralize the sodium hydroxide. It was then air-dried for another 24 hours to remove excess water content (Figure 1).

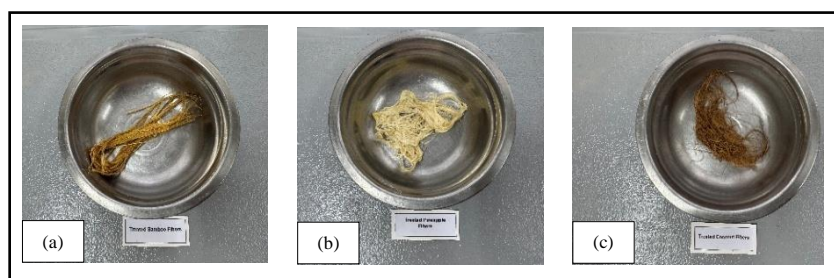


Figure 1. Treated bamboo fibers (a); treated pineapple fibers (b); treated coconut fibers (c)

## 2.3 Laboratory Tests

### 2.3.1 Morphological Characterization

The surface morphology of untreated and mercerized fibers was examined using a Scanning Electron Microscope, JEOL, JSM IT-200. The specimens

were sputter-coated with gold to a thickness of 10  $\mu\text{m}$  to prevent the agglomeration of electrostatic charges in the electron beam (Nusantara *et al.*, 2025). Additionally, the tests conducted included imaging and elemental analysis of the fibers. An accelerating voltage of 10.0 kV was used to collect SEM micrographs of untreated and treated fibers at a magnification of  $\times 1000$ . Through SEM, morphological changes such as fiber diameter distribution and porosity were observed.

### 2.3.2 Chemical Characterization

The chemical composition of fibers was determined using Fourier Transform Infrared Spectroscopy, Shimadzu IR Tracer 100. A total of 3 samples per fiber were employed during the testing. The spectrum analysis displayed the transmittance percentage and wavenumber in  $\text{cm}^{-1}$  where the absorption critical peaks of fibers is ascribed to a distinctive functional group (Tavadi *et al.*, 2025).

### 2.3.3 Single Fiber Tensile Strength Test

The tensile strength of single strand lignocellulosic fibers was conducted in consonance with the comprehensive procedure outlined in ASTM D3822. It is performed using a Universal Testing Machine, Shimadzu AGS-X Series. Table 1 displayed the physical properties of lignocellulosic fibers. Three replicates of each fiber type were produced and these fibers were subjected to a crosshead speed of 5mm/min using a 5000N load cell.

Table 1: Physical properties of fibers

Lignocellulosic Fibers	Thickness (mm)	Width (mm)	Gauge Length (mm)
Bamboo	1	1	100
Pineapple	1	1	100
Coconut	1	1	100

## 2.4 Statistical Techniques

### 2.4.1 Principal Component Analysis

This is a multivariate statistical technique widely applied in the interpretation of FTIR spectroscopy data to identify patterns, similarities, and differences among samples based on their spectral features. In the context of fiber characterization, PCA helps in transforming the complex, overlapping

infrared absorption spectra into a simplified visual representation that captures the essential chemical variations between untreated and treated lignocellulosic fibers.

#### 2.4.2 One-Way Analysis of Variance (ANOVA)

This is a statistical test used to determine whether there are significant differences among the means of independent groups. It separates the total variation in the data into between-group variation and within-group variation and compares them using an F-ratio.

The Grand Mean ( $\bar{X}$ ) represents the overall average of all data points from all groups combined. It is calculated using Equation 1:

$$\bar{X} = \frac{\sum_{i=1}^k \sum_{j=1}^{n_i} X_{ij}}{N} \quad (1)$$

Where  $X_{ij}$  = j-th observation in the  $i^{th}$  group,  $n_i$  is the number of observations in  $i^{th}$  group,  $k$  is the total number of groups, and  $N = \sum_{i=1}^k n_i$  is the total number of all observations.

The between-group sum of squares measures the variation between group means and the grand mean as shown in Equation 2:

$$SS_B = \sum_{i=1}^k n_i (\bar{X}_i - \bar{X})^2 \quad (2)$$

Additionally, the within-group sum of squares is calculated using Equation 3:

$$SS_W = \sum_{i=1}^k \sum_{j=1}^{n_i} (X_{ij} - \bar{X}_i)^2 \quad (3)$$

Moreover, the F-value compares the between-group and within-group mean squares as shown in Equation 4:

$$F = \frac{MS_B}{MS_W} \quad (4)$$

### 3.2 Post Hoc Test (Turkey's Honest Significant Difference)

This statistical method compares all possible pairs of group means and uses a single critical value to infer whether the difference between any two means is statistically significant.

The test statistic is computed using Equation 5:

$$HSD = q \times \sqrt{\frac{MS_{within}}{n}} \quad (5)$$

Where  $q$  denotes the studentized range statistic,  $MS_{within}$  is the mean square within from ANOVA, and  $n$  is the number of observations per group.

## 3. Results and Discussion

### 3.1 SEM Analysis

Figure 2 illustrates the surface morphology of untreated bamboo, coconut, and pineapple fibers. Figure 2a shows crack propagation and the presence of cylindrical holes in bamboo fibers. This correlates with the study of Chakkour *et al.* (2023), where the vascular bundles display crack propagation due to fiber debonding, swollen fibers, and weak fibrils. Similarly, figure 2b displays intercellular gaps and a porous structure that comprises a large void fraction in the cell wall. This is ascribed to the presence of globular protrusions that disrupt the polymer chains and crystalline regions of coconut fibers (Fu *et al.*, 2023). Moreover, Figure 2c exhibits interface crack propagation, delamination, fiber fracture, and visible voids in the fiber's microstructure. This is attributed to fiber-matrix debonding and void formation, which are commonly seen on the fracture surface morphology of vascular bundles (Gnanasekaran *et al.*, 2021).

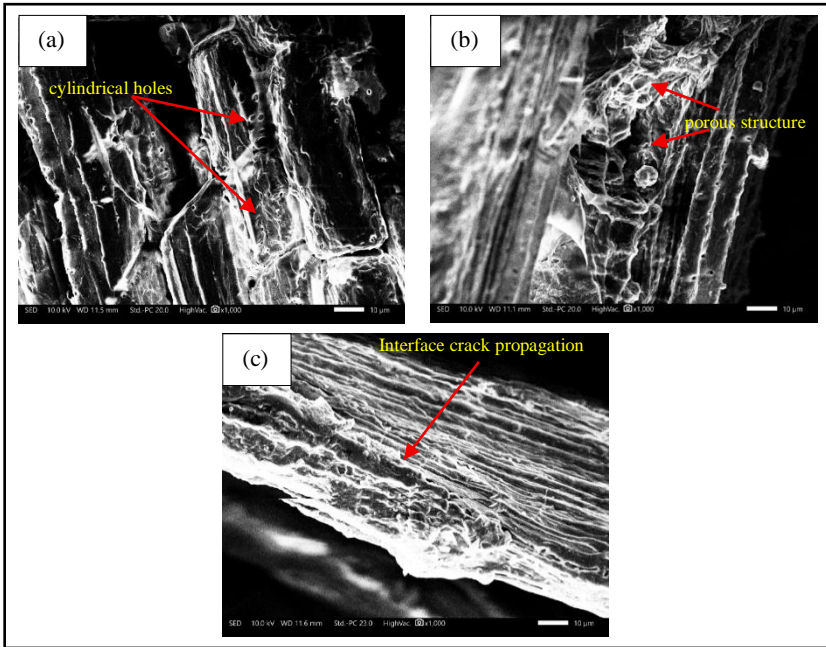


Figure 2. Surface morphology of untreated bamboo fibers (a), surface morphology of untreated coconut fibers (b), surface morphology of untreated pineapple fibers (c)

Figure 3 elucidates the mercerized bamboo, coconut, and pineapple fibers. Figure 3a demonstrated an enhanced interfacial bonding of bamboo fibers since the NaOH reacts well with the hydroxyl groups of the vascular bundles, thereby cementing their cellular structure. Additionally, the fiber surface revealed an interlocking adhesion of the matrix resin as the surface morphology changes. Similarly, Figure 3b exhibited an improvement of interfacial adhesion through the removal of hemicelluloses, surface impurities, and inorganic particles, with substantial increase in crystallinity and cellulose composition on the surface morphology of coconut fibers based on the results of its FTIR spectrum. This is attributed to the hydrophilic behavior of cellulose microfibrils that reacts well with NaOH treatment, increasing the fibers' adhesion force in the mechanical interlocking of vascular bundles (Bharath *et al.*, 2023). Moreover, figure 3c displayed an enhanced adhesion of the polymer matrix while maintaining the fiber geometry and cellulosic composition of pineapple leaf fibers. The NaOH treatment increased the surface roughness through the removal of non-cellulosic components such as lignin and hemicellulose, and this is ascribed to the reduction of pore configurations on the vascular bundles (Akbar and Gnanamoorthy, 2024).

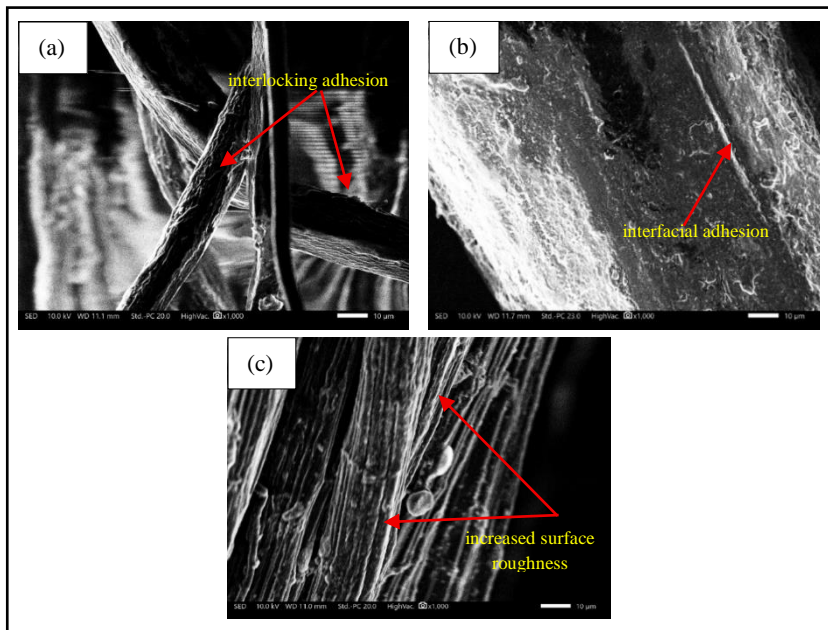


Figure 3. Surface morphology of treated bamboo fibers (a), surface morphology of treated coconut fibers (b), surface morphology of treated pineapple fibers (c)

### 3.2 Simulated Histograms of Fiber Diameter Distribution and Porosity of Untreated and Treated Fibers

The results of the simulated diameter distribution histograms revealed that mercerization significantly reduced the mean diameters of fiber groups (Figure 4). Bamboo fibers reduced from 220  $\mu\text{m}$  to 180  $\mu\text{m}$  (18.18%), pineapple fibers reduced from 150  $\mu\text{m}$  to 115  $\mu\text{m}$  (23.33%), and coconut fibers reduced from 260  $\mu\text{m}$  to 240  $\mu\text{m}$  (7.69%). This percentage reduction in mean diameters reflect the removal of amorphous lignin and other surface impurities as elucidated by latest literature (Rai and Chandrashekar, 2025). Moreover, the 6% alkali treatment also showed significant percent reduction in porosity as shown in Figure 5. Bamboo fibers reduced from 38.7% to 25.3%, pineapple fibers reduced from 43.3% to 30%, and coconut fibers reduced from 52.0% to 48.0%. This percentage reduction corresponded to enhanced interfacial bonding due to the densification of voids in the fibers' microstructure.

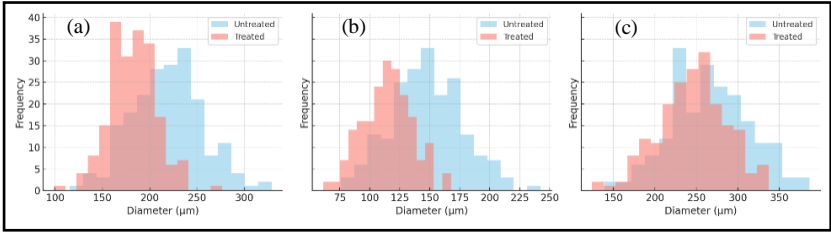


Figure 4. Untreated and treated bamboo fiber diameter distribution (a), untreated and treated pineapple fiber diameter distribution (b), untreated and treated coconut fiber diameter distribution (c)

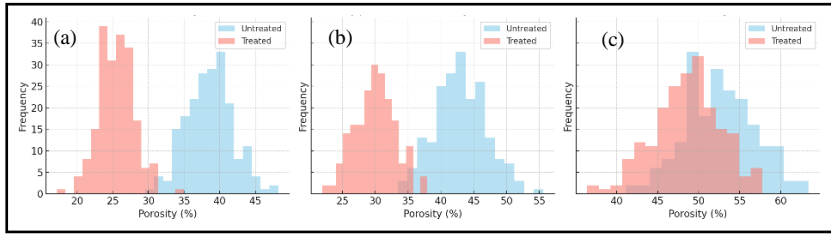


Figure 5: Porosity of untreated and treated bamboo fibers (a), porosity of untreated and treated pineapple fibers (b), porosity of untreated and treated coconut fibers (c)

### 3.3 FTIR Spectrum Analysis

Figure 6 illustrates the FTIR spectrum of untreated and mercerized pineapple fibers within the range of  $500$  to  $4000\text{ cm}^{-1}$ . The current spectra showed strong absorption bands of different functional groups at varying frequencies of  $3356\text{ cm}^{-1}$ ,  $2924\text{ cm}^{-1}$ ,  $1747\text{ cm}^{-1}$ ,  $1153\text{ cm}^{-1}$ , and  $1026\text{ cm}^{-1}$  (Figure 6). The region at  $3356\text{ cm}^{-1}$  revealed bands of carboxylic acid O-H stretching of  $\alpha$ -cellulose - the primary constituent of pineapple leaf fibers which is in correlation to the previous study (Sumiati and Suryadi, 2023). However, the peak at  $3356\text{ cm}^{-1}$  of the treated pineapple fibers showed a decreased intensity due to the reduction in hydrogen bonding intensity as the hemicellulose and lignin content were partially removed during mercerization. This change exposed more cellulose hydroxyl groups, improving the fiber's crystallinity and interfacial bonding with polymer matrices in potential composite applications. Conversely, the wavenumber at  $2924\text{ cm}^{-1}$  corresponded to C-H stretching in microcrystalline cellulose as supported by previous literature (Lee *et al.*, 2020). The slight increase in wavenumber from  $2915$  to  $2924\text{ cm}^{-1}$  is caused by the partial degradation of hemicellulose and amorphous components, resulting in improved surface morphology. Moreover, the peak at  $1747\text{ cm}^{-1}$

is linked to C=O stretch which is a characteristic of the carbonyl group. After mercerization, there's a minor decrease in intensity due to the partial removal of lignin and hemicellulose components. Additionally, the cellulose absorption peak at  $1153\text{ cm}^{-1}$  is linked to C-O/C-C stretch. The increased wavenumber for the treated fiber corresponded to the more ordered cellulose structure with minimal amorphous lignin components. Furthermore, the distinctive absorption band of  $1026\text{ cm}^{-1}$  corresponded to the C-O/C-C stretch of the  $\beta$ -1, 4-glycosidic linkage (Chaves *et al.*, 2024). The slight change in wavenumber from  $1024$  to  $1026\text{ cm}^{-1}$  in mercerized fibers is linked to enhanced cellulose exposure while retaining the fundamental polysaccharide backbone.

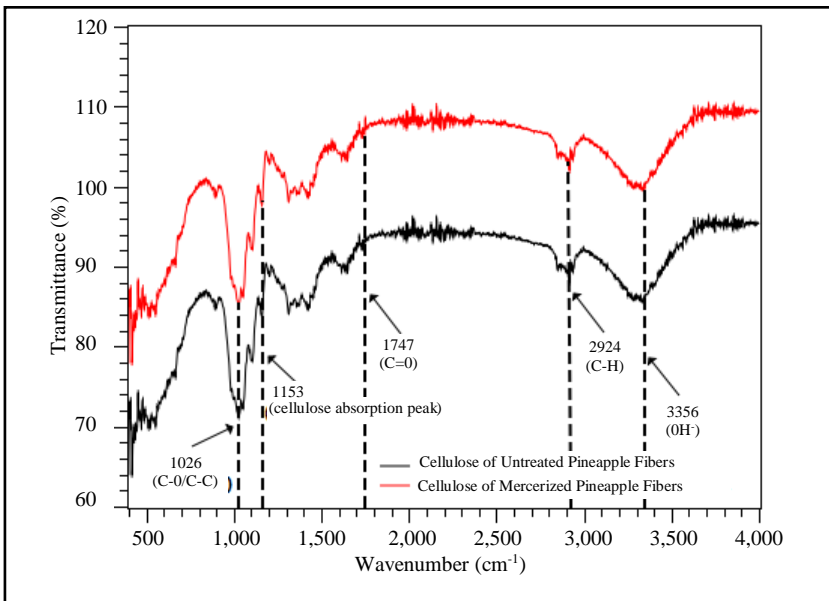


Figure 6. FTIR spectrum of cellulose from untreated and mercerized pineapple fibers

Figure 7 shows the plotted normalized transmission carrying frequency and wavenumber of untreated and treated bamboo fibers. The critical peaks suggest the presence of O-H group that contains cellulose, C-H and C=O group that comprises pectin and hemicellulose, and C-O/C-C group that contains amorphous lignin. The broad transmission band in the region of  $3389\text{ cm}^{-1}$  is attributed to O-H stretching vibrations in cellulose, which is the fundamental component of bamboo fibers as supported by previous study (Geremew *et al.*, 2024). Additionally, the mercerized cellulose contained more O-H groups of  $\alpha$ -cellulose than in untreated bamboo fibers. Conversely, the

strong band at  $2916\text{ cm}^{-1}$  corresponds to C-H stretching vibrations as supported by earlier literature (Biswas *et al.*, 2022). The minimal improvement in wavenumber from  $2912$  to  $2916\text{ cm}^{-1}$  is caused by the removal of extractives, surface waxes, and amorphous hemicelluloses. On the other hand, the critical absorption peak at  $1640\text{ cm}^{-1}$  is correlated to unconjugated carbonyl stretching (C=O) in hemicellulose as elucidated in a previous study (Wu *et al.*, 2023). The slight improvement in wavenumber is ascribed to the removal of the cleavage of ester linkages between hemicellulose and lignin. Moreover, the cellulose absorption peak at  $1163\text{ cm}^{-1}$  is linked to C-O/C-C stretch in amorphous lignin (Rasheed *et al.*, 2020). The shift to  $1163\text{ cm}^{-1}$  after mercerization denoted a relative increase in cellulose structure. Furthermore, the wavenumber at  $1030\text{ cm}^{-1}$  corresponded to C-O/C-C vibrations in cellulose and varying polysaccharides. The increase in wavenumber for treated fibers reflects greater exposure of cellulose chains.

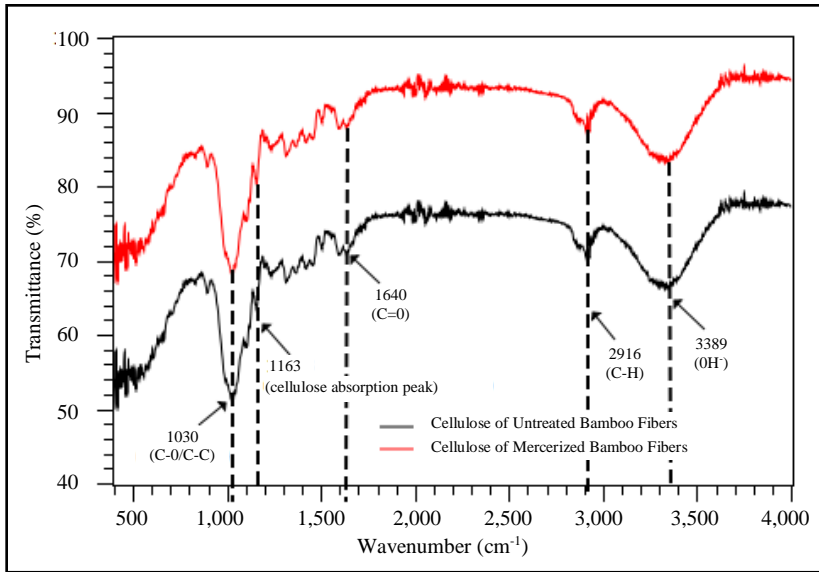


Figure 7. FTIR spectrum of cellulose from untreated and mercerized bamboo fibers

Figure 8 elucidated the FTIR spectrum absorption peaks of untreated and mercerized coconut fibers. The peak at  $3339\text{ cm}^{-1}$  is ascribed to O-H groups from cellulose hydroxyls. The change in wavenumber from  $3335$  (untreated) to  $3339\text{ cm}^{-1}$  (treated) is caused by the modification of intermolecular hydrogen bonds as the amorphous hemicellulose and lignin were partially removed. The peak at  $2930\text{ cm}^{-1}$  is linked to asymmetric stretch of C-H groups as supported by previous study (Bharath *et al.*, 2023). The slight improvement

in wavenumber from 2921 (untreated) to 2930  $\text{cm}^{-1}$  (treated) is ascribed to the removal of surface extractives and amorphous polysaccharides, resulting in a cleaner cellulose-rich surface. Conversely, the peak at 1754  $\text{cm}^{-1}$  is attributed to CO bonds as supported by previous literature (Bright *et al.*, 2021). A shift to 1754  $\text{cm}^{-1}$  after mercerization is due to the removal of non-cellulosic components. Moreover, the cellulose absorption peak at 1193  $\text{cm}^{-1}$  corresponded to C-O/C-C asymmetric stretching in glycosidic linkages of polysaccharides. The upward shift to 1193  $\text{cm}^{-1}$  after treatment is due to the relative increase in crystalline cellulose.

Furthermore, the peak at 1035  $\text{cm}^{-1}$  is ascribed to lignin peak band due to C-O/C-C stretch in-plane aromatic vibration as supported by earlier literature (Ramkumar *et al.*, 2022). The change in wavenumber from 1032 (untreated) to 1035  $\text{cm}^{-1}$  (treated) is due to increased exposure of cellulose chains, resulting in higher crystallinity and reduced interference from disordered regions of lignin and hemicellulose. This increase in crystallinity, a significant implication of our research, enhances the potential applications of mercerized coconut fibers in various industries.

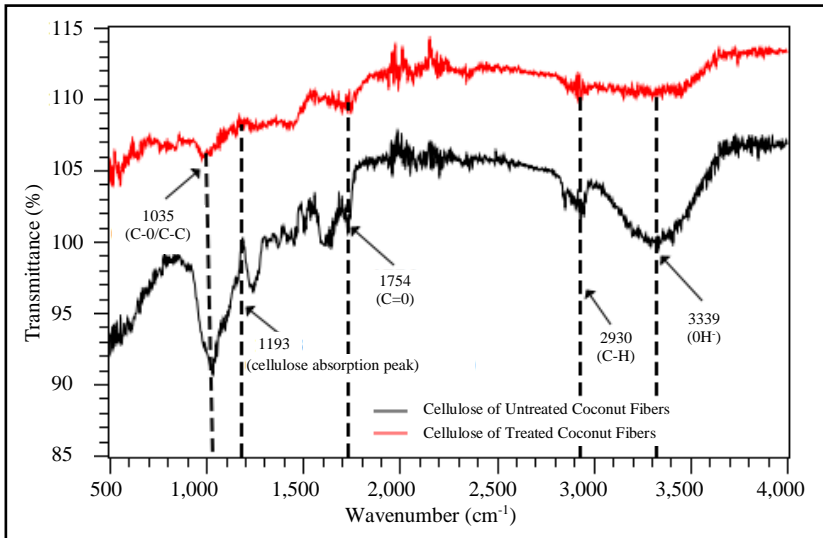


Figure 8: FTIR spectrum of cellulose from untreated and mercerized coconut fibers

### 3.4 Statistical Analysis of the FTIR Data of Untreated and Treated Fibers

The PCA score plot revealed a well-defined clustering among fiber groups, and a clear distinction between treated and untreated samples within each cluster. The first principal component (PC1) accounts for approximately 99.95% of the total variance. This means that the mercerization caused significant alterations in the chemical structure among fiber groups. The directional chemical shift of treated fibers toward higher PC1 values is ascribed to the relative increase in intensity of O-H and C-O-C bonds, implying partial delignification. Conversely, the second component (PC2) contributed approximately 0.05% of the total variance, reflecting almost negligible inter-fiber variations. Moreover, Figure 7 elucidated that the O-H ( $3350\text{--}3390\text{ cm}^{-1}$ ) and C-O/C-C ( $1030\text{--}1150\text{ cm}^{-1}$ ) absorption bands exerted the greatest influence on the first principal component (PC1), confirming their dominant role in differentiating treated from untreated fibers. Among the samples, bamboo fibers exhibited the highest spectral shifts, indicating stronger chemical modification, followed by pineapple and coconut fibers.

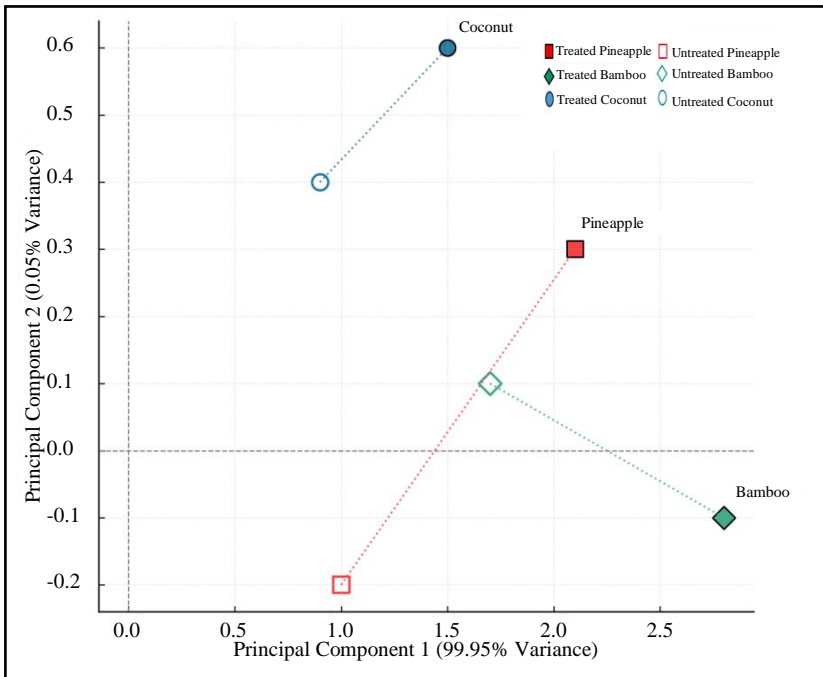


Figure 9: Principal Component Analysis Score Plot of Untreated and Treated Fibers

### 3.5 Tensile Strength Analysis

The stress-strain curve illustrates steeper slopes and higher endpoints for treated fibers, confirming their improved strength and ductility after mercerization (Figure 10). Among the fiber groups, treated bamboo fibers yield the highest strain of 2.5%, suggesting that mercerization has improved its ductility and mechanical strength. Treated bamboo fibers exhibited the highest tensile strength of 23.69 MPa, signifying a 90.43% increase in tensile strength (Figure 11). As per the results of the FTIR analysis, treated bamboo fibers contain high cellulose content as its absorption peak increases from 3335 to 3339 $\text{cm}^{-1}$ , hence the removal of amorphous hemicellulose and lignin. This is also supported by the enhanced interfacial bonding of bamboo fibers since the NaOH reacts well with the hydroxyl groups of the vascular bundles, thereby cementing their cellular structure (Figure 3a). Conversely, treated pineapple fibers displayed the second highest tensile strength of 20.10 MPa, implying a 178.39% increase in tensile strength. This is because the absorption band of treated pineapple fibers increases from 3348 to 3356 $\text{cm}^{-1}$  which exposes more cellulose hydroxyl groups, hence improved crystallinity and interfacial bonding with polymer matrices. This is also supported by the enhanced adhesion of the polymer matrix due to the reduction of pore configurations on the vascular bundles (Figure 5c). Moreover, treated coconut fibers exhibited the lowest tensile strength of 2.04 MPa, yielding a 10.87% increase in tensile strength. This is because coconut fibers contain mostly non-cellulosic matrix such as hemicellulose, surface impurities, and lignin which compromise its mechanical strength (Vieira *et al.*, 2024)

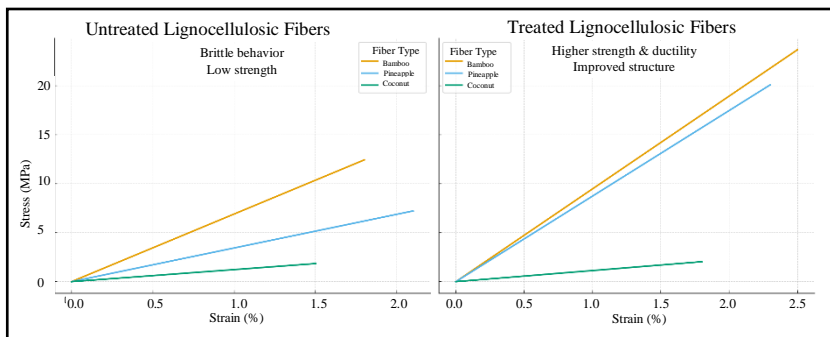


Figure 10: Comparison of stress-strain curves of untreated and treated fibers

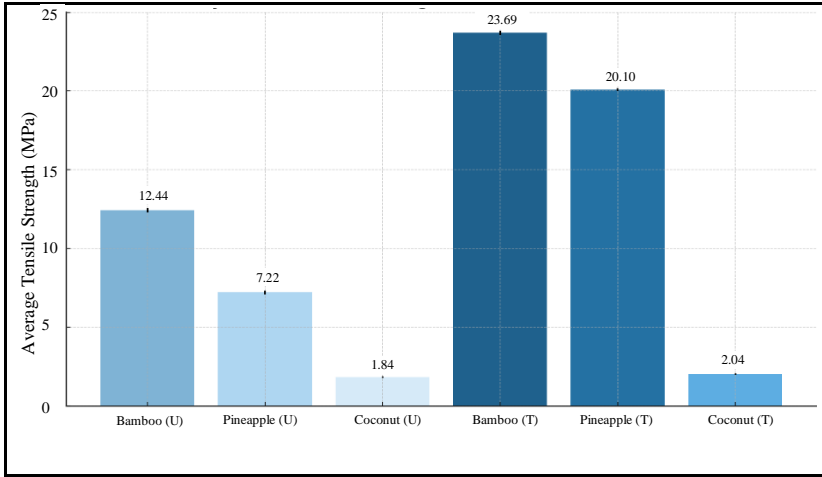


Figure 11: Average tensile strength results of untreated and treated fibers

### 3.6 One-Way ANOVA and Post-Hoc Test Results

The null hypothesis in Table 2 denotes that there is no significant correlation in mean tensile strength among the treated and untreated fiber groups. Since the F-value ( $F=18,825.93$ ) is greater than the F-statistic ( $F_{crit}=3.11$ ), the null hypothesis is rejected. Hence, the results are statistically significant ( $p<0.05$ ). Moreover, the low within-group variance of 0.0068 revealed good consistency and reliability.

Table 2: One-Way Anova Results

Source of Variation	Sum of Squares (SS)	Degree of Freedom (df)	Mean Square (MS)	F	Fcritical ( $p<0.05$ )
Between Groups	1277.13	5	255.43	18825.93	3.11
Within Groups	0.081	12	0.0068	—	—
Total	1277.21	17	—	—	—

Since the ANOVA results are significant, a post hoc test was performed to ascertain which treatment groups differ from varying treatment groups (Table 3). The honest significant difference (HSD) critical value of 0.19 was computed based on the ANOVA results, wherein this value elucidated that any mean difference greater than the HSD critical value is statistically significant ( $p < 0.05$ ). The post hoc test revealed that treated bamboo fibers responded

more effectively to mercerization than pineapple and coconut fibers, obtaining the highest tensile strength of 23.69 MPa.

Table 3: Post-Hoc Test Results

Comparison	Mean Difference ( $\Delta$ )	Significant (>0.19)?	Interpretation
Bamboo (Treated) vs Bamboo (Untreated)	11.25	Yes	Alkali treatment greatly increased tensile strength.
Pineapple (Treated) vs Pineapple (Untreated)	12.88	Yes	Enhanced tensile strength after treatment.
Coconut (Treated) vs Coconut (Untreated)	0.20	Slightly significant	Small but measurable improvement.
Bamboo (Treated) vs Pineapple (Treated)	3.59	Yes	Bamboo (treated) stronger than pineapple (treated).
Bamboo (Untreated) vs Pineapple (Untreated)	5.22	Yes	Untreated bamboo stronger than untreated pineapple.
Pineapple (Untreated) vs Coconut (Untreated)	5.38	Yes	Untreated pineapple much stronger than untreated coconut.
Coconut (Untreated) vs Bamboo (Treated)	21.85	Yes	Treated bamboo exhibited huge difference in tensile strength.
Coconut (Treated) vs Pineapple (Treated)	18.06	Yes	Coconut remains weakest.
Coconut (Treated) vs Bamboo (Untreated)	10.40	Yes	Untreated bamboo still stronger than treated coconut.

#### 4. Conclusion and Recommendation

The study uncovered a novel approach through a diversified analysis on the significant correlation of 6% NaOH treatment to the chemical structure, surface morphology, and physical characteristics of fibers such as mean diameter and porosity. The FTIR spectra of treated fibers demonstrated a reduction and disappearance of C=O and C–O–C bands, and the relative increase of O-H stretching associated with cellulose hydroxyl groups. This chemical delignification resulted in enhanced cellulose crystallinity due to its

ordered molecular chains of cellulose, leading to a remarkable improvement in tensile strength. Correspondingly, the SEM micrographs exhibited an enhanced fiber-matrix adhesion and mechanical interlocking on the surface morphology of the fibers' vascular bundles. This is supported by the reduction of mean diameter and porosity of fibers due to the dissolution of non-cellulosic layers, hence improved mechanical strength. Additionally, the 6% NaOH solution is a sustainable pretreatment concentration for natural fiber reinforcement in biocomposite and geotechnical applications. Hence, this study revealed that bamboo fibers demonstrated the most favorable properties for potential biocomposite and geotextile applications after 6% NaOH treatment, followed by pineapple and coconut fibers. Moreover, these mercerized fibers can serve as reinforcement for practical use in applications such as erosion control mats, biodegradable geotextiles, natural fiber composites, and other eco-sustainable engineering materials. Furthermore, this study recommended the durability testing of fibers under environmental conditions, including ultraviolet radiation, moisture and humidity exposure, abrasive weathering, and biological and microbial degradation.

## 5. Acknowledgement

Gratitude is extended to the Center for Sustainable Polymers at Mindanao State University–Iligan Institute of Technology for accommodating laboratory requests. Appreciation is also conveyed to the Civil Engineering Laboratory Office of the University of Science and Technology of Southern Philippines – Cagayan de Oro for permitting the execution of laboratory tests related to the mercerization of fibers.

## 6. References

- Akbar, A., & Gnanamoorthy, R. (2024). Characterization of Treated and Untreated Pineapple Leaf Fiber for Engineering Applications. *Materials Circular Economy*, 6(1), 18. <https://doi.org/10.1007/s42824-024-00116-x>
- Balbin, D.J., Padilla, D., Retamal, J.B., Abana, E., & Ventura, J. (2022, June). PALFNet: a soil erosion control geotextile using pineapple leaf fiber. In *International Conference on Structural Engineering and Construction Management* (pp. 1-14). Cham: Springer International Publishing. [https://doi.org/10.1007/978-3-031-12011-4\\_1](https://doi.org/10.1007/978-3-031-12011-4_1)

Bawadi, N.F., Basri, N.S.C., Mansor, A.F., & Hamid, S.H. (2025, April). Sustainable soil solutions: the role of coir in geotechnical engineering. In IOP Conference Series: Earth and Environmental Science (Vol. 1495, No. 1, p. 012011). IOP Publishing. <https://doi.org/10.1088/1755-1315/1495/1/012011>

Bharath, K.N., Puttegowda, M., Mavinkere Rangappa, S., Basavarajappa, S., Siengchin, S., Khan, A., & Gorbatyuk, S.M. (2023). Study of treatment effect on the Cocos nucifera lignocellulosic fibers as alternative for polymer composites. *Journal of Natural Fibers*, 20(1), 2134257. <https://doi.org/10.1080/15440478.2022.2134257>

Biswas, S., Rahaman, T., Gupta, P., Mitra, R., Dutta, S., Kharlyngdoh, E., ... & Das, M. (2022). Cellulose and lignin profiling in seven, economically important bamboo species of India by anatomical, biochemical, FTIR spectroscopy and thermogravimetric analysis. *Biomass and Bioenergy*, 158, 106362. <https://doi.org/10.1016/j.biombioe.2022.106362>

Bright, B.M., Joseph Selvi, B., Abu Hassan, S., Mustapha Jaafar, M., Siengchin, S., Mavinkere Rangappa, S., ... & Padmavathy, S.R. (2021). Characterization of chemically treated new natural cellulosic fibers from peduncle of *Cocos nucifera* L. Var typica. *Polymer Composites*, 42(12), 6403-6416.

Caingles, V.K.S., & Lira, A.Y. (2025). Assessment of Pineapple and Coconut Fibers (PICONET) as Natural Geotextile in Mitigating Soil Erosion. *Philippine Journal of Science*, 154(3), 687-695. <https://doi.org/10.56899/154.03.12>

Chakkour, M., Moussa, M.O., Khay, I., Balli, M., & Zineb, T.B. (2023). Effects of humidity conditions on the physical, morphological and mechanical properties of bamboo fibers composites. *Industrial Crops and Products*, 192, 116085. <https://doi.org/10.1016/j.indcrop.2022.116085>

Chaves, D.M., Araújo, J.C., Gomes, C.V., Gonçalves, S.P., Figueiro, R., & Ferreira, D.P. (2024). Extraction, characterization and properties evaluation of pineapple leaf fibers from Azores pineapple. *Heliyon*, 10(4). <https://doi.org/10.1016/j.heliyon.2024.e26698>

dos Santos, A.J., Ribeiro, M.M., Corrêa, A.D.C., Rodrigues, J.D.S., Silva, D.S., Junio, R.F., & Monteiro, S.N. (2024). Morphological, chemical and mechanical properties of hybrid polyester composites reinforced with bamboo fibers and kaolin waste. *Journal of Materials Research and Technology*, 30, 1-15. <https://doi.org/10.1016/j.jmrt.2024.03.003>

Dessalegn, Y., Singh, B., van Vuure, A.W., Rajhi, A.A., Ahmed, G.M.S., & Hossain, N. (2022). Influence of age and harvesting season on the tensile strength of bamboo-fibre-reinforced epoxy composites. *Materials*, 15(12), 4144. <https://doi.org/10.3390/ma15124144>

Fu, S., Wu, H., Zhu, K., Zhao, Z., & Liang, Z. (2023). The unique morphology of coconut petiole fibers facilitates the fabrication of plant composites with high impact performance. *Polymers*, *15*(9), 2200. <https://doi.org/10.3390/polym15092200>

Gnanasekaran, S., Nordin, N.I.A.A., Hamidi, M.M.M., & Shariffuddin, J.H. (2021). Effect of Alkaline treatment on the characteristics of pineapple leaves fibre and PALF/PP biocomposite. *Journal of Mechanical Engineering and Sciences*, *15*(4), 8518-8528. <https://doi.org/10.15282/jmes.15.4.2021.05.0671>

Hawanis, H.S.N., Ilyas, R.A., Jalil, R., Ibrahim, R., Majid, R.A., & Ab Hamid, N.H. (2024). Extraction and characterization of morphological, physical, physiochemical, thermal, and chemical composition of five bamboo malaysian species. *Cellulose*, *31*(13), 7941-7952. <https://doi.org/10.1007/s10570-024-06090-6>

Hindi, J., Muralishwara, K., & Gurumurthy, B.M. (2025). Comparative analysis of physical, morphological, tensile and thermal stability characteristics of raw and alkali treated novel *Tinospora cordifolia* natural fiber. *Scientific Reports*, *15*(1), 1-12. <https://doi.org/10.1038/s41598-025-03627-y>

Holanda, F.S.R., Vidal Santos, L.D., Melo, J.C.R., Pedrotti, A., Sussuchi, E.M., Griza, S., ... & Nascimento, B.L. (2024). Influence of Sodium Hydroxide Treatment on *Typha domingensis* Fibers for Geotextile Manufacturing. *ACS omega*, *9*(52), 51040-51051. <https://doi.org/10.1021/acsomega.4c05602>

Kumar, S. (2023). Study of Geosynthetics and use of Non-Woven Green Geocomposite Blanket for Erosion Control and Slope Protection for Embankment. *International Research Journal of Engineering and Technology (IRJET)*, *10*(4), 1657-1663. <https://www.irjet.net/archives/V10/i4/IRJET-V10I4249.pdf>

Lee, C.H., Khalina, A., Lee, S.H., Padzil, F.N.M., & Ainun, Z.M.A. (2020). Physical, morphological, structural, thermal and mechanical properties of pineapple leaf fibers. *Pineapple Leaf Fibers: Processing, Properties and Applications*, 91-121.

Li, L., Peng, T., & Zhang, Q. (2025). Durability of chemically treated coir geotextiles coated with epoxy resin in different degradation environments. *Acta Geotechnica*, 1-17.

Nguyen, T.T., & Indraratna, B. (2023). Natural fibre for geotechnical applications: concepts, achievements and challenges. *Sustainability*, *15*(11), 8603. <https://doi.org/10.3390/su15118603>

Nusantara, F., Suryanto, H., Aminuddin, A., Puspitasari, P., Aldin, A., Renandito, M. P., & Osman, H. (2025). Morphology and Structure of Bagasse Fiber after Chemical Treatment. In *IOP Conference Series: Earth and Environmental Science* (Vol. 1439, No. 1, p. 012035). IOP Publishing.

- Pinka, H.F., Wibowo, D.E., & Munawir, R. (2021). The Effect of Reinforcement of Bamboo Matting, Bamboo Grids, and Geotextiles on Non-Woven Increasing the Carrying Capacity of Clay Soil Using the Loading Test. In IOP Conference Series: Earth and Environmental Science (Vol. 832, No. 1, p. 012008). IOP Publishing. <https://doi.org/10.1088/1755-1315/832/1/012008>
- Rai, P. S., Unnikrishnan, S., & Chandrashekar, A. (2025). Influence of alkali treatment on physiochemical and morphological properties of palmyra fibers. *Industrial Crops and Products*, 224, 120298. <https://doi.org/10.1016/j.indcrop.2024.120298>
- Ramkumar, T., Hariharan, K., Selvakumar, M., & Jayaraj, M. (2022). Effect of various surface modifications on characterization of new natural cellulosic fiber from coconut tree secondary flower leaf stalk fiber (CSF). *Journal of Natural Fibers*, 19(16), 13362-13375. <https://doi.org/10.1080/15440478.2022.2091715>
- Rasheed, M., Jawaid, M., Karim, Z., & Abdullah, L.C. (2020). Morphological, physiochemical and thermal properties of microcrystalline cellulose (MCC) extracted from bamboo fiber. *Molecules*, 25(12), 2824. <https://doi.org/10.3390/molecules25122824>
- Sachin Chakravarthy, G., GuhaRay, A., & Kar, A. (2021). Experimental investigations on strength and durability of alkali-activated binder-treated natural jute geotextile. *International Journal of Geosynthetics and Ground Engineering*, 7(4), 97. <https://doi.org/10.1007/s40891-021-00341-3>
- Sebastain, S., & Divya, P.V. (2024). Natural fibres: a sustainable material for geotextile applications. *Indian Geotechnical Journal*, 54(3), 1056-1072. <https://doi.org/10.1007/s40098-023-00862-w>
- Sumiati, T., & Suryadi, H. (2023). Morphological, characterization and FTIR analysis of delignified pineapple leaves as raw material for cellulose production. In IOP Conference Series: Earth and Environmental Science (Vol. 1160, No. 1, p. 012072). IOP Publishing. <https://doi.org/10.1088/1755-1315/1160/1/012072>
- Tanasá, F., Nechifor, M., Ignat, M.E., & Teacă, C.A. (2022). Geotextiles—a versatile tool for environmental sensitive applications in geotechnical engineering. *Textiles*, 2(2), 189-208. <https://doi.org/10.3390/textiles2020011>
- Tavadi, A.R., Basheer, D., Melese, K.G., Kumaresan, K., Mohan, N., Kerur, M.R.H., & Shashidhara, L.C. (2025). Experimental analysis of mechanical properties and FTIR analysis of areca fiber-reinforced epoxy composites incorporating Al<sub>2</sub>O<sub>3</sub>. *Journal of Industrial Textiles*, 55, 15280837241313217. <https://doi.org/10.1177/15280837241313217>

Singh, B., Dessalegn, Y., Wakjira, M.W., Girma, C., Rajhi, A.A., Duhduh, A.A. (2023). Characterization of bamboo culm as potential fibre for composite development. *Materials*, 16(14), 5196. <https://doi.org/10.3390/ma16145196>

Tulin, E.P.B., & Bande, M.M. (2018). Agroecological Assessment of Different Cultural Practices of Pineapple, *Ananas comosus*, (Linn) Mer. (Var. Red Spanish) for Sustainable Fiber Production in Geo-Textile Industry in Balete, Aklan. *International Journal of Environmental and Rural Development*, 9(1), 18-24.

Vieira, F., Santana, H.E., Jesus, M., Mata, F., Pires, P., Vaz-Velho, M., ... & Ruzene, D.S. (2024). Comparative study of pretreatments on coconut fiber for efficient isolation of lignocellulosic fractions. *Sustainability*, 16(11), 4784. <https://doi.org/10.3390/su16114784>

Wu, J., Zhong, T., Zou, Y., Li, J., Zhao, W., & Chen, H. (2023). Microstructure, chemical composition and thermal stability of alkali-treated bamboo fibers and parenchyma cells: effects of treatment time and temperature. *Cellulose*, 30(3), 1911-1925. <https://doi.org/10.1007/s10570-022-04995-8>